jet INTL JOURNAL OF ELECTRONICS AND TELECOMMUNICATIONS, 2022, VOL. 68, NO. 4, PP. 775-781
Manuscript received October 28, 2021; revised November 2022. DOI: 10.24425/ijet.2022.143885

# Modeling and Design of a Highly Efficient Switch-Mode RF/Microwave Power Amplifier Based-on Microstrip Bandpass Filter

Farzad Moloudi, Omid Eslamipour, and Ali Khoshnoud

***Abstract*—This paper presents a broadband Switch-Mode Power Amplifier (SMPA) using a Band-Pass Filter (BPF) at the Output Matching Network (OMN). The proposed SMPA integrates a microstrip BPF as an output impedance matching network to significantly reduce the final circuit size. The microstrip lines of the filter simultaneously play the role of filtering and impedance matching. This proposed method reduces the size of the PA and reduces the power dissipation as much as possible. The BPF is placed at the output of the circuit using microstrip lines and the RT Duroid 6006 substrate. This BPF covers a wide bandwidth ranging from $3.0\ GHz$ *to* $4.4\ GHz$. Simulation results show $9-14\ dB$ gain with $44-56.6\ \%$ drain efficiency ($DE\ \%$), and the output power of $39-41.3\ dBm$ would be achieved across the frequency band from $3.0\ GHz$ to $4.4\ GHz$.**

***Keywords*—broadband; band-pass filter (BPF); switch-mod;, power amplifier (PA); matching network (MN)**

## I. Introduction

THE rapid growth of wireless telecommunication technology has led to the design and implementation of transmitter and receiver circuits in fewer comparisons and maximum performance. It is also necessary to consider the battery life of portable devices in these designs. The Power Amplifier (PA) has the highest power dissipation in the transmitter architecture, which should be designed to be an optimal and low loss. Power added efficiency (PAE%), gain (dB), output power (dBm), linearity, and bandwidth (BW) are the primary metrics of RF PAs. The high efficiency of an RF PA indicates a small amount of dissipated power and a high amount of linearity. Linear performance is required to create maximum efficiency and output power in a PA. However, novel generation systems, including WiMAX, $4G$, and $5G$, definitely require more bandwidth due to the broader spectrum allocation.

High-efficiency RF Switch-Mode Power Amplifiers (SMPAs) [1-3] can be designed based on the conduction angle of the transistors (active device), which are classified into Class-D [4], Class-E [5], Class-F [6], and Class-J [7], etc. The SMPAs use a harmonic tuning method to increase performance, which causes the voltage and current waveform in the drain terminal to be half-sinusoidal. The common SMPA is shown in Figure 1. A PA consists of several parts: transistor, input/output matching network (MN), gate bias, and drain bias. The bias network (at the gate and drain terminal) applies the desired voltage to the transistor to the circuit with a fixed value. It should be noted that 50-ohm filter inputs and outputs will be considered as standard.

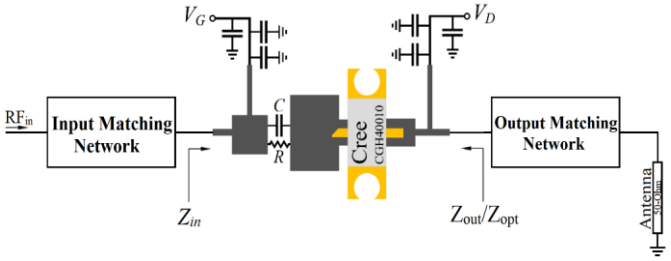


Fig. 1. Schematic of the new generation of SMPA

SMPA bias circuits operate so that the reactance of the supply lines ($L$ or $RFC$) is so large that the current passing through it is constant and unchanged. MNs at the input/output of the PA are responsible for impedance matching and power transmission. However, MNs play a significant role in suppressing and controlling the harmonics created (due to nonlinear elements). Also, BPFs [8] and LPF [9] can be used in input/output MNs. Also, the quality factor ($Q$) of the resonant circuit at the Output Matching Network (OMN) of the PA is so significant that the output current and voltage waveforms are sinusoidal. In the SMPA, when the transistor (Switch) is OFF, the current in the drain is zero, and when the transistor (Switch) is ON, the voltage in the drain is zero, and the current flows through the switch and the MN. This condition causes there to be no overlap between the voltage and current waveforms.

In recent years, many methods have been reported to increase the efficiency and bandwidth of SMPA [10-12] designs. To increase the bandwidth of the PA, the designers have focused more on the OMN part. To reduce the final size of the PA, the impedance matching operation at the OMN can be performed by the filter itself [13]. Using a two-pole evanescent-mode (EVA) cavity filter in the OMN can have a very sharp frequency response (high-Q) but with limited bandwidth in a single frequency. However, the designer must also consider the complexity of implementing an EVA cavity filter. Reference [14] presents a broadband high-efficiency PA using good BPF responses in OMN. In [15], a tunable line at the BPF input increases bandwidth and sets the most optimal impedance. By adjusting the input impedance of the BPF, the bandwidth can be increased to some extent, but this method causes nonlinear effects in PA. In other words, it increases the overlap between the voltage and current waveforms in the transistor drain.

This paper presents a broadband RF SMPA to achieve high efficiency and high power using a micro-strip BPF. Instead of

Farzad Moloudi, Omid Eslamipour are with University of Kurdistan, Iran (email: f.moloudi@uok.ac.ir, o.eslamipour@uok.ac.ir).

Ali Khoshnoud is with Iran University of Science and Technology, Iran (email: a_khoshnoud@elec.iust.ac.ir).

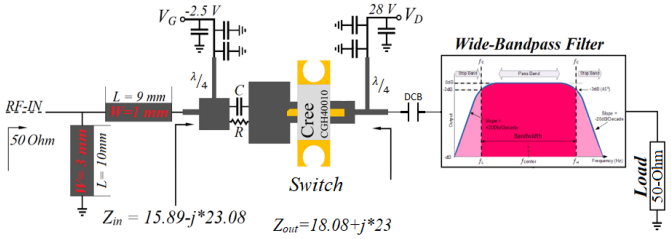


Fig. 2. The proposed schematic of SMPA using input/output MN

matching the impedance of the transistor to the impedance of 50 ohms, a broadband BPF is used, which is connected directly to the drain and reduces the final size of the PA. In other words, the microstrip BPF is embedded in the OMN. It is noteworthy that eliminating additional circuits (such as separate impedance matching) dissipated less power in the OMN. Also, reducing the complexity of the circuit causes the nonlinear effects to be significantly reduced, reducing the overlap of the voltage and current drain waveforms. This paper shows that the OMN is an RF PA is not always two separate parts.

## II. Design of Broadband Power Amplifier using Band-Pass Filter as Output Matching Network

### A. Power Amplifier Design

The most challenging part of the SMPA design is the part of the IMN at the input/output of the circuit. As usual, the transmitter architecture considers 50-ohm input and output impedances to design a filter (BPF, LPF, etc.). However, when in PA design is used filter as impedance matching in the OMN, the input impedance of the filter is less than 50-ohms ($Z \neq 50\Omega$). Figure 2 clearly shows the proposed schematic with the GaN transistor (CGH40010F model) and matches the input and output impedances.

According to Figure 2, the quarter-wave line ($\lambda/4$) is used for bias drain and gate. The length ($L$) and width ($W$) of the $\lambda/4$ line in the drain terminal is 9 $mm$ and 2 $mm$, respectively, and the $L$ and $W$ of this line in the gate terminal is 9 $mm$ and 1 $mm$, respectively. Also, six bypass capacitors with 10 $uF$, 10 $nF$, and 10 $pF$ are used for decoupling. The capacitor ($C = 10\ pF$) and resistance ($R = 120\ \Omega$) considered in the transistor gate are added as an increase in the stability of the PA.

The voltage applied to the drain and gate of the transistor is 28 volts and $-2.5$ volts, respectively, to operate the PA in switch mode. The negative voltage at the gate is due to the GaN transistor fabrication technology, the depletion type. The depletion-mode transistor usually is on and is turned off with a negative voltage relative to the drain and source electrodes. The negative voltage ($-2.5$ volts) applied to the transistor gate can affect the DC load-line curve and the output impedance of the transistor (drain impedance). Drain impedance ($Z_{load}$) and gate impedance ($Z_{in}$) for maximum efficiency and output power using load-pull simulation are shown in Figure 3.

For our design, the maximum power impedance selected [see smith chart], whose input ($Z_{in}$) and output ($Z_{load}$) impedances are: $Z_{in} = 15.89 - j23.08\ \Omega$, and $Z_{load} = 18.08 + j23\ \Omega$, respectively.

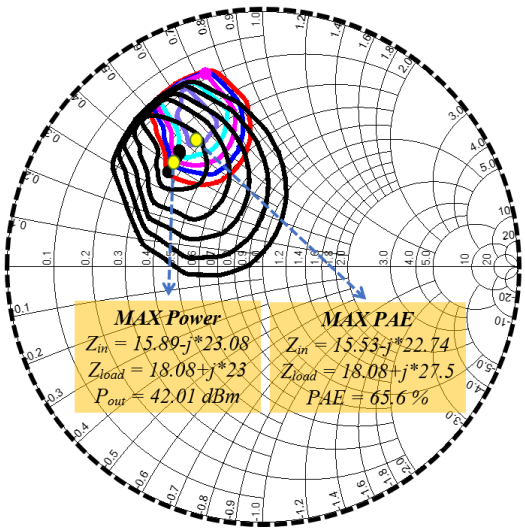


Fig. 3. Input and output impedances using load-pull simulation

As shown in Figure 3, PA can achieve 42 $dBm$ (15.8 $W$) power and 65.6 % efficiency in exchange for these impedances obtained from the load-pull. As a result, the impedance converts at the input ($Z_{in} = 15.89 - j23.08)\Omega$ is done through two microstrip lines, with lengths of 9 $mm$ and 10 $mm$ and widths of 1 $mm$ and 3 $mm$, respectively. However, the output impedance ($Z_{load}$) is converted to optimal impedance ($18.08 + j23)\Omega$ using a broadband microstrip BPF, described in the following subsection.

## III. Broadband Band-Pass Filter (BPF) Design

Figure 4 represents the proposed broadband BPF that plays the role of matching the output impedance of the PA. This filter will convert the drain transistor's 50-ohm impedance antenna (load) to optimal ($Z_{optimum}$).

This research aims to design an SMPA without a fixed MN that provides maximum performance in a wide frequency range. For this purpose, a BPF is designed using microstrip lines to match the output impedance. The broadband BPF structure is designed and simulated with microstrip lines on the Rogers RT Duroid 6006 substrate with $\varepsilon r = 6.15$, $h = 1.27\ mm$, and $tan\ \delta = 0.0027$. The $L$ and $W$ of the BPF are in millimeters, which is shown in Figure 4 in full detail. As it is known, five parallel stubs with almost the same length and width have been used. The input filter with an impedance of $(18.08 + j23)\Omega$ will be connected to the transistor (drain), and the output of the filter with an impedance of 50-ohms will be connected to the antenna. The design of a broadband microstrip transient filter that covers the entire bandwidth of 3 to 4.4 GHz is proposed.

The equivalent structure of the short-circuit stub microstrip bandpass filter is shown in Figure 5. This filter consists of parallel short circuit stubs and interface lines with a quarter wavelength in the central frequency.

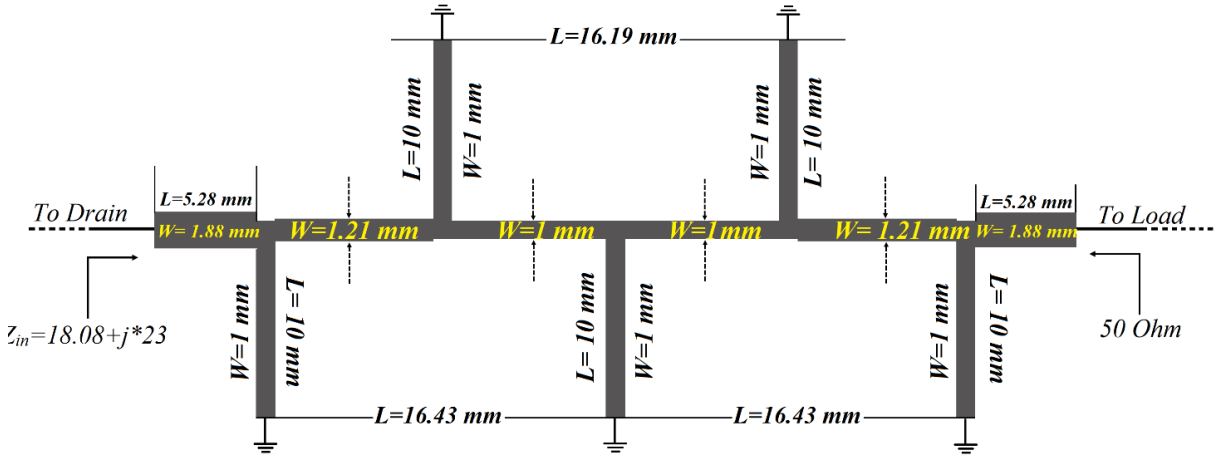


Fig. 4. The proposed broadband BPF uses a microstrip line

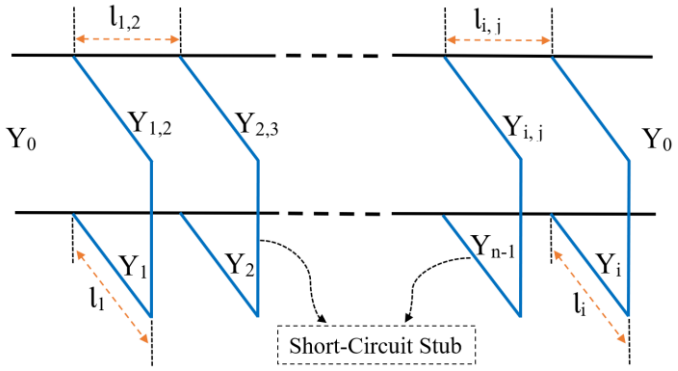


Fig. 5. Microstrip bandpass filter with short-circuit subs

In this structure, the characteristic impedance and the characteristic admittance are equal to 50-Ω and 50-℧, respectively. For designing the proposed BPF, the values of the elements for the prototype are chosen as [15]: $g_0 g_6 = 1$, $g_1 g_5 = 1.146$, $g_2 g_4 = 1.371$, and $g_3 = 1.97$. For 5th Order quarter-wavelength short-circuited stubs (n=5), characteristic admittances of the stub lines and the characteristic admittances of the connecting lines are marked with $Y_i (i = 1\ to\ n)$ and $Y_{i,i+1} (i = 1\ to\ n-1)$, respectively. The following equation should be used to calculate the transmission line characteristic admittances of BPF [15],

$$Y_{i,i+1} = Y_0 \left(\frac{J_{i,i+1}}{Y_0}\right) \qquad for\ i = 1\ to\ n-1 \tag{1}$$

where $J_{i,i+1}$ is the reverse J, calculated in equations (2) and (3),

$$\frac{J_{1,2}}{Y_0} = g_0 \sqrt{\frac{g_1}{g_2}} h \tag{2}$$

$$\frac{J_{n-1,n}}{Y_0} = g_0 \sqrt{\frac{g_1 g_{n+1}}{g_2 g_{n-1}}} h \tag{3}$$

although $J_{i,i+1}$ can be calculated as follows,

$$\frac{J_{i,i+1}}{Y_0} = \frac{g_0 g_1}{\sqrt{g_i g_{i+1}}} h \qquad for\ i = 2\ to\ n-2 \tag{4}$$

where, the constant $h$ is a dimensionless constant whose value can be considered 2 ($h = 2$). Stub $Y_1$ and $Y_{n-1}$ admittances can be calculated as follows,

$$Y_1 = Y_0 g_0 \left(1 - \frac{1}{2} h\right) tan\Theta g_1 + \left(N_{n-1,n} - \frac{J_{n-1,n}}{Y_0}\right) Y_0 \tag{5}$$

$$Y_{n-1} = tan\Theta Y_0 \left(g_{n-1} g_n - g_0 g_1 {}^{h}/_{2}\right) + \left(N_{n-1,n} - \frac{J_{n-1,n}}{Y_0}\right) Y_0 \tag{6}$$

where,

$$\theta = \left(1 - \frac{\text{Fractional Bandwidth}}{2}\right) \frac{\pi}{2} \tag{7}$$

also, Fractional Bandwidth $(FBW)$ is calculated as follows,

$$(FBW) = \frac{f_2 - f_1}{f_0} \quad with\ f_0 \frac{f_1 + f_2}{2} \tag{8}$$

where $f_1$, $f_2$, and $f_0$ are the upper frequency, the lower frequency, and the central frequency of the filter response, respectively. In the following, other stub BPF admittances can be calculated,

$$Y_i = Y_0 \left(N_{i-1,i} + N_{i,i+1} - \frac{J_{i-1,i}}{Y_0} - \frac{J_{i,i+1}}{Y_0}\right) \quad for\ i = 2\ to\ n-1 \tag{9}$$

$$Y_{i,i+1} = Y_0 \left(\frac{J_{i,i+1}}{Y_0}\right) \quad for\ i = 1\ to\ n-1 \tag{10}$$

$$N_{i,i+1} = \sqrt{\left(\frac{J_{i,i+1}}{Y_0}\right)^2 + \left(\frac{h g_0 g_1 tan\theta}{2}\right)^2} \quad for\ i = 1\ to\ n-1 \tag{11}$$

In the following, equation 12 can also calculate the width of microstrip lines,

$$\frac{w}{h} = \frac{2}{\pi} \left\{ \left({60\pi^2}/{Z_c \sqrt{\varepsilon_r}} - 1\right) - ln + \frac{\varepsilon_r - 1}{2\varepsilon_r} \left[ ln\left({60\pi^2}/{Z_c \sqrt{\varepsilon_r}} - 1\right) + 0.39 + \frac{0.61}{\varepsilon_r} \right] \right\} \tag{12}$$

TABLE I.

SPECIFICATIONS OF BPF AS OMN

| Parameter | Specifications |
|---|---|
| Insertion loss @2.8 GHz | **< -10 dB** |
| Insertion loss @4.5 GHz | **< -10 dB** |
| Fractional-BW | **63.4%** |
| Center Frequency (GHz) | **4.1** |
| Input Impedance | **18 Ω** |
| Output Impedance | **50 Ω** |
| S-Parameter ($S_{11}$) | **<-15 dB** |

where,

$$Z_c = \frac{\eta}{\sqrt{\varepsilon_{re}}}\left\{\frac{W}{h} + 1.393 + 0.677ln\left(\frac{W}{h} + 1.444\right)\right\}^{-1} \quad with \quad \varepsilon_{re} = 6.15 \tag{13}$$

where $\eta$ is the wave impedance in free space, which is calculated as follows,

$$\eta = \sqrt{\frac{\mu_0}{\varepsilon_0}} = 376.73\ \Omega = 120\pi\ \Omega \quad with \begin{cases} \mu_0 = 4\pi \times 10^{-7}\ H/m \\ \varepsilon_0 = 8.854 \times 10^{-12} \end{cases} \tag{14}$$

where $\varepsilon_0$ is the permittivity constant in free space and $\mu_0$ is the permeability constant in free space.

The ideal electrical model for the filter is based on short-wavelength stub resonators generalized by microstrip lines. The broadband BPF specifications are summarized in Table I.

Figure 6 shows the frequency response of the broadband BPF in ADS and CST environments when the input impedance is $(18.08 + j23)\Omega$ ohms. In total bandwidth $(2.8\ GHz\ to\ 5.4\ GHz)$, the value of parameter $S11$ is more petite than $-12$. Connecting this filter to a transistor drain without a separate impedance matching network can reduce the valuable bandwidth. The reduction in bandwidth can be the nonlinear effects of the transistor and the RF power transmitted through the BPF. Also, changing the input impedance of the filter at different frequencies can be effective in reducing the valuable bandwidth.

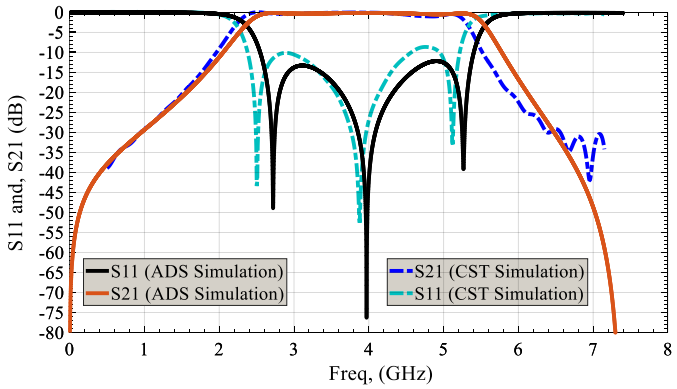


Fig. 6. The wide-band BPF S-parameter

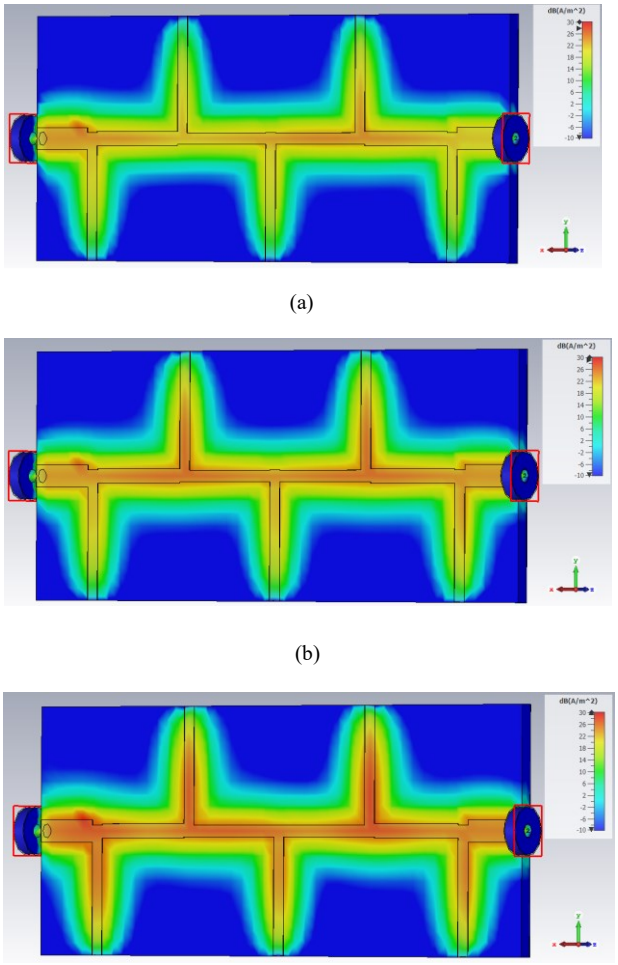

(a) (b) (c)

Fig. 7. The current density in frequency: (a) 3.0 GHz (b) 3.8 GHz and (c) 4.4 GHz

Also, to verify the simulation results in a schematic environment (ADS), the bandpass filter is simulated in a magnetic environment (CST studio), presented. The current density at the three different filter frequencies is shown in Figure 7. According to the results obtained in Figure 7, the electric field distribution between the stubs and the microstrip lines at different frequencies is visible. The value of the electric field density increases with the frequency value; near the first microstrip line, this value is higher.

Figure 8 illustrates the magnitude of the Electric Field distribution at the central frequency (3.8 GHz) of the BPF. The electric field is transferred from port 1 (Input port) to port 2 (Output port) in the filter's central frequency.

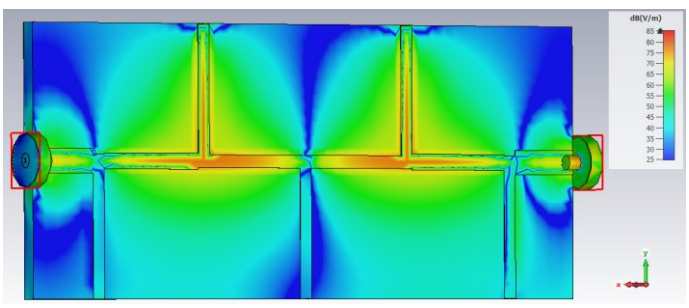

Fig. 8. The electric field distribution results of BPF at 3.8 GHz

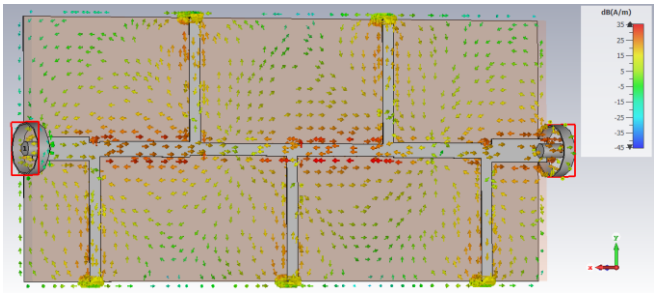

(a)

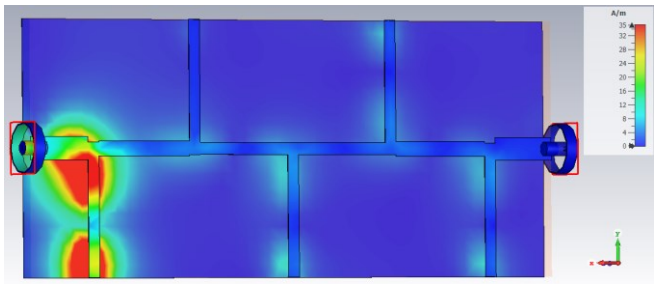

(b)

Fig. 9. The surface currents distribution results at (a) pass-band zone (3.8 GHz) and (b) band stop zone (7.5 GHz)

The surface currents distribution results of the BPF at pass-band region (3.8 $GHz$) and bandstop region (7.5 $GHz$) are shown in figure 9 to show the BPF operation. In the passband, the 3.8 $GHz$ signal can be transferred to the output port of a bandpass filter with minimal losses. On the other hand, the signal band at 4 $GHz$ is suppressed at the beginning of the input filter in the stopband. The electric field distribution simulation results show that in the passband, the filter has a good performance.

## IV. Simulation Results

This section presents the results obtained from the SMPA simulation using a broadband BPF at the OMN with ADS and CST. In all the simulations performed in this PA, the input power signal ($RF_{in}$) value of 30 $dBm$ is selected, equal to 1 $watt$. The proposed PA, as a switch-mode, should have no overlap between current and voltage waveforms to maximize output power and efficiency. Figure 10 shows the voltage and current waveforms of the drain at frequencies 3 $GHz$, 3.7 $GHz$, and 4.4 $GHz$.

In Figure 10, it is clear that there is no overlap between the current and voltage waveforms in the drain, which in turn reduces the RF power losses. The current drain transistor and the whole frequency band are minimum and maximum 1.35 $A$ to 1.45 $A$, respectively.

Figure 11 also represented the gain and output power simulation results versus the input RF power ($dBm$) across the BPF bandwidth (3 $GHz$ $to$ 4.4 $GHz$). This figure's maximum and minimum gain values are 9 $dB$ to 11.5 $dB$ at 4.2 $GHz$ and 3 $GHz$, respectively. According to Figure 11, the maximum gain of 11.4 $dB$ and output power 41.4 $dBm$ in 4.2 $GHz$ and 4.4 $GHz$, respectively.

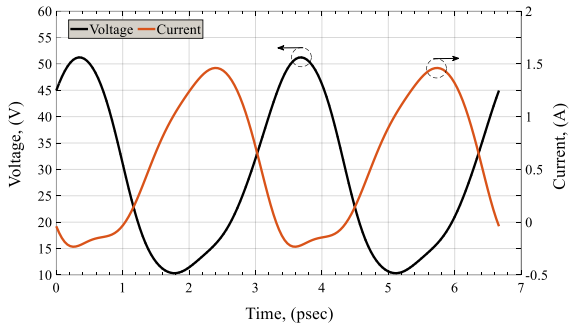


(a)

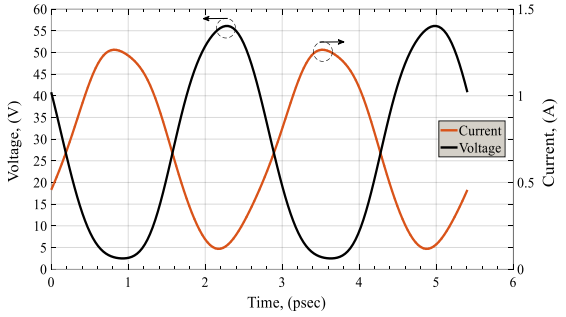


(b)

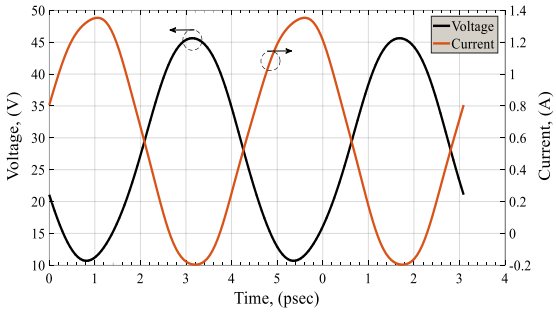


(c)

Fig. 10. Simulation of voltage and current waveforms PA at (a) 3.0 GHz (b) 3.7 GHz (c) 4.4 GHz

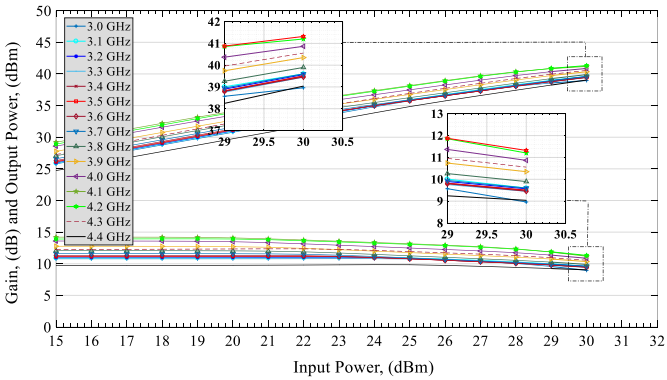


Fig. 11. Simulated gain and output power versus input power (dBm)

Figure 12 shows the simulated results under the linearity criterion, including the fundamental harmonic output power and the third-order intermodulation component. As shown in Figure 12, the $OIP3$ point is extracted by changing the input power signal, which results in a measurement of $OIP3$ of about 60 $dBm$. According to the results, this SMPA can be compared with other previous works focused on linearization methods.

TABLE II
PERFORMANCE SUMMARY AND COMPARISONS WITH OTHER PAS

| Ref. | | Freq (GHz) | PAE (%) | DE (%) | $P_{out}$ (dBm) | Gain (dB) | Filter Type | Year |
|---|---|---|---|---|---|---|---|---|
| [8] | | 2-2.4 | - | 69-78.2 | 39-40.4 | 9.8-10.6 | Microstrip BPF | 2020 |
| [9] | | 1.7-2.6 | - | 65-78 | 39.7-42.1 | 9.1 -10.1 | Microstrip LPF | 2019 |
| [13] | | 3.05 | 65 | 72 | >40 | >10 | Microstrip BPF | 2013 |
| [14] | | 2.45 | 69.8 | - | 40.1 | 11.8 | Microstrip BPF | 2014 |
| **Our design** | **Circuit Simulation** | **3 – 4.4** | **43 – 53.4** | **44 – 56.6** | **39 - 41.3** | **9 - 14** | **Microstrip BPF** | **2022** |
| | **EM-Simulation** | | **42.1 – 52.6** | **43.7 – 55.6** | **39 - 41.15** | **9 – 13.4** | | |

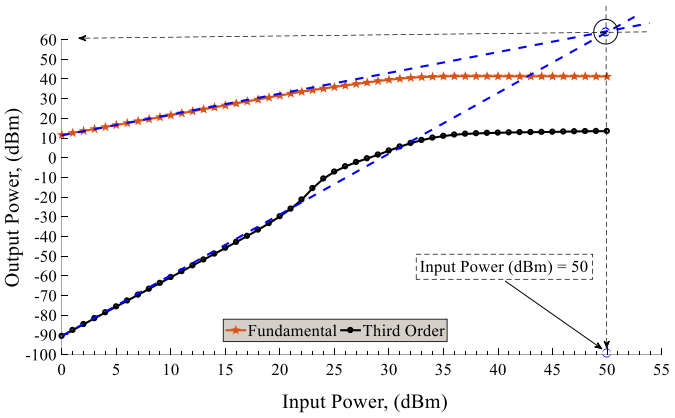


Fig. 12. Simulated linearity performance

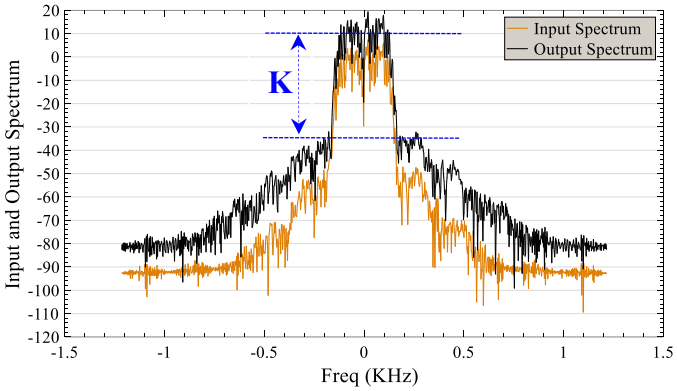


Fig. 13. Simulation of the ACPR at central frequencies (3.8 GHz)

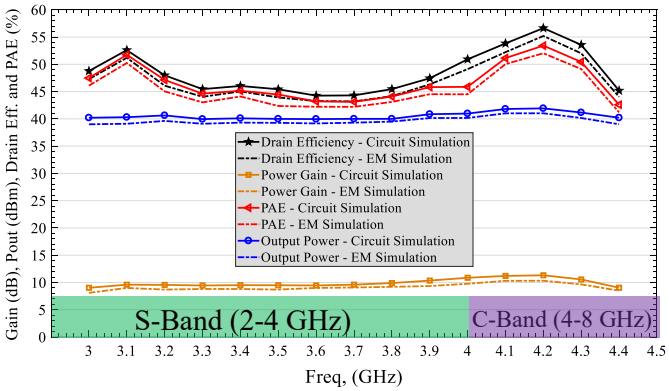


Fig. 14. Simulated performances of the PA versus frequency.

Figure 13 shows the simulated output spectrum at a central frequency $(3.8\,GHz)$ with an input power of 30 dBm. The simulated output spectrum is obtained using a 16-QAM (Quadrature Amplitude Modulation) signal at the central frequency. The value of Adjacent Channel Power Ratio (ACPR) across the entire bandwidth is approximately $-30$ to $-32\,dBc$. Reducing the switching behavior of the transistor at high frequency has caused the upper half-band to improve linearity [see K factor in Figure 13].

Figure 14 illustrates the overall performance of the SMPA at a glance, where all the fundamental parameters such as power, gain, and efficiency in a PA design in terms of bandwidth frequencies are considered. These results are presented in both schematic and electromagnetic (EM simulation) environments.

The EM simulation results are very similar to the circuit simulation results. The maximum efficiencies at $4.2\,GHz$ are $56.63\%$ and $53.42\%$, respectively. Also, the maximum gain and output power at $4.2\,GHz$ is $11.32\,dB$ and 41.32 dBm, respectively. It is clear from the figure that SMPA performance is more stable in the second half of the S-Band frequency range. But at the beginning of the C-Band frequency range, the SMPA performance is unstable, with the difference that the highest amount of efficiency, gain and output power is in this range.

Finally, all the simulated results in this research are summarized in Table 2. Compared to other similar designs, this design offers excellent performance in terms of the frequency range and the most critical parameters of PA (output power, gain, efficiency, and frequency bandwidth).

## V. CONCLUSIONS

This paper presents a highly efficient SMPA with the ability to amplification power and filter. An SMPA with a broadband BPF in the OMN is designed and simulated using microstrip lines. In this design, the GaN CGH40010F transistor is used as a power device or switch. The broadband BPF in the OMN is connected directly to the transistor drain terminal and forms the IMN. As a result, the proposed SMPA includes a BPF as part of its output matching network, optimizing circuit performance and reducing PA circuit size. Using this filter in OMN provides 3 to $4.4\,GHz$ bandwidth in the PA. This SMPA can provide $44\% - 56.6\%$ efficiency, $39\,dBm - 41.3\,dBm$ output power, and $9\,dB - 14\,dB$ gain in this frequency bandwidth.

## REFERENCES

[1] A. Grebennikov, NO. Sokal, and MJ. Franco. "Switchmode RF and microwave power amplifiers," 2nd ed., Academic Press; 2021.

[2] A. Barakat, M. Thian, and V. Fusco, "A High-Efficiency GaN Doherty Power Amplifier with Blended Class-EF Mode and Load-Pull Technique". *IEEE Transactions on Circuits and Systems II: Express Briefs*, 65:151–5, 2018. https://doi.org/10.1109/TCSII.2017.2677745

[3] C. Liu, and QF. Cheng, "Analysis and Design of High-Efficiency Parallel-Circuit Class-E/F Power Amplifier," IEEE Transactions on Microwave Theory and Techniques, 67:2382–92, 2019. https://doi.org/10.1109/TMTT.2019.2902548

[4] H. Kobayashi, JM. Hinrichs, and PM. Asbeck, "Current-Mode Class-D Power Amplifiers for High-Efficiency RF Applications," *IEEE Transactions on Microwave Theory and Techniques*, 49:2480–5, 2001. https://doi.org/10.1109/22.971639.

[5] NO. Sokal, AD. Sokal, "Class E-a new class of high-efficiency tuned single-ended switching power amplifiers," *IEEE Journal of solid-state circuits*; 10:168–76, 1975. https://doi.org/10.1109/JSSC.1975.1050582

[6] FH. Raab, "Class-F Power Amplifiers with Maximally Flat Waveforms". *IEEE Transactions on Microwave Theory and Techniques*, 45:2007–12, 1997. https://doi.org/10.1109/22.644215

[7] CS. Cripps, "RF Power amplifiers for wireless communications,". 2nd ed. Boston: MA, Artech House; 2006.

[8] Z. Su, C. Yu, B. Tang, and Y. Liu, "Bandpass Filtering Power Amplifier with Extended Band and High Efficiency," *IEEE Microwave and Wireless Components Letters*, 30:181–4, 2020. https://doi.org/10.1109/LMWC.2020.2966067

[9] Z. Zhuang, Y. Wu, Q. Yang, M. Kong, and W. Wang, "Broadband Power Amplifier Based on a Generalized Step-Impedance Quasi-Chebyshev Lowpass Matching Approach," *IEEE Transactions on Plasma Science*; 48:311–8, 2020. https://doi.org/10.1109/TPS.2019.2954494

[10] F. Moloudi, H. Jahanirad, "Broadband class-E power amplifier design using tunable output matching network". *AEU-International Journal of Electronics and Communications*, 118:153142, 2020.

[11] F. Moloudi, O. Eslamipour, "Wide-band switching-mode power amplifier using varactor-based reconfigurable output matching network," *AEU-International Journal of Electronics and Communications*, 132:153647, 2021.

[12] D. Wisell, D. Rönnow, and P. Händel, "A technique to extend the bandwidth of an RF power amplifier test bed," *IEEE Transactions on Instrumentation and Measurement*, 56:1488–94, 2007. https://doi.org/10.1109/TIM.2007.900101

[13] K. Chen, J. Lee, WJ. Chappell, and D. Peroulis, "Co-Design of highly efficient power amplifier and high-Q output bandpass filter". *IEEE Transactions on Microwave Theory and Techniques*, 61:3940–50, 2013. https://doi.org/10.1109/TMTT.2013.2284485

[14] L. Gao, XY. Zhang, S. Member, S. Chen, and Q. Xue, "Compact power amplifier with bandpass response and high efficiency". *IEEE Microwave and Wireless Components Letters*, 24:707–9, 2014. https://doi.org/10.1109/LMWC.2014.2340791

[15] J. Hong, and MJ. Lancaster, "Microstrip Filters for RF/Microwave". vol. 7. 2001.